

SUPPLEMENTARY INFORMATION

QM/MM Simulations as an Assay for Carbapenemase Activity in Class A β -Lactamases

Ewa I. Chudyk,^a Michael A. L. Limb,^a Charlotte Jones,^a James Spencer,^b Marc W. van der Kamp,^{a*} Adrian J. Mulholland^{a*}

^aSchool of Chemistry, University of Bristol, United Kingdom

^bSchool of Cellular and Molecular Medicine, University of Bristol, United Kingdom

Methods

Starting structures for modeling β -lactamase deacylation

The protein/ligand complexes in the acylenzyme state were prepared based on the available crystal structures (see Table S1). The following β -lactamases were setup for QM/MM calculations: SFC-1, KPC-2, NMC-A, SME-1, TEM-1, SHV-1, BlaC, CTX-M-16. TEM-1 was prepared with acylenzymes of two different ligands, benzylpenicillin and meropenem, and the other β -lactamases were set up as meropenem acylenzyme complexes. The AMBER 12 package¹ with the AMBER ff12SB (protein) or the General Amber Force Field² (ligand) was used for MM calculations. Partial charges for the free and covalently bound ligand were obtained by RESP fitting of HF/6-31G* calculations performed using Gaussian09³ and RED-IV through the RED Server⁴ (<http://q4md-forcefieldtools.org/REDS/>). Protonation states for ionizable residues were calculated using PROPKA 3.1,⁵ suggesting residues were in their standard states. Histidine tautomers were selected based on optimum hydrogen bonding patterns. (Unphysical pK_a values of over 10 were found for some Asp residues in several structures, however, it was found the source of these abnormal values was due to close contacts formed with nearby residues. These steric clashes were relieved upon an initial minimization of the structures during equilibration.) Hydrogen atoms were added accordingly by the AmberTools program tLEAP. Crystallographic water molecules were deleted from the structures, apart from the deacylating water molecule present in the active site. Each system was solvated with a TIP4P-Ew⁶ water box extending at least 10 Å from any protein heavy atom, and sodium ions were added to neutralize the systems.

The crystal structure of the SFC-1 acylenzyme was represented by the Glu166Ala mutant (PDB: 4EV4⁷). The reverse mutation to Glu166 was performed based on the Ser70Ala mutant complex with meropenem (PDB: 4EUZ⁷). For BlaC, the meropenem acylenzyme structure was used (PDB: 3DWZ⁸). For SHV-1 (PDB: 2ZD8⁹) only the conformation of meropenem with the carbonyl oxygen in the oxyanion hole was considered for deacylation calculations. The structure of TEM-1 with meropenem was set up with the carbonyl oxygen in the oxyanion hole, obtained by brief restrained modelling based on the crystal structure of the imipenem acyl-enzyme replaced with meropenem (PDB: 1BT5¹⁰) (where the carbonyl oxygen is placed outside of the oxyanion hole). The apoenzyme structures of KPC-2 (PDB: 2OV5¹¹), NMC-A (PDB: 1BUE¹²), SME-1 (PDB: 1DY6¹³), CTX-M-16 (PDB: 1YLW¹⁴) were aligned with the SFC-1 structure in acylenzyme (PDB: 4EV4⁷), and the coordinates of the antibiotic were used to build their meropenem acylenzymes in apo structures. In addition, TEM-1 was also set up with benzylpenicillin, using the Glu166Asn mutant structure in the acylenzyme state (PDB: 1FQG¹⁵); Glu166 was restored by extension of the main chain of the residue.

QM/MM setup and equilibration

For the QM/MM calculations, the SCC-DFTB method was used for the QM region. For the systems with meropenem, the QM region consisted of 41 atoms and 3 link atoms (Figure S1). The Glu166 side chain up to the CG atom and the deacylating water molecule were treated QM. The acylated meropenem was included in the QM region from CB of Ser70 up to the S atom, as the remaining group is positioned further from the active site residues (mostly exposed to solvent). For the complexes with benzylpenicillin, the QM region consisted of 54 atoms and 2 link atoms, with the entire antibiotic included in the QM region (from CB of Ser70; Figure S1).

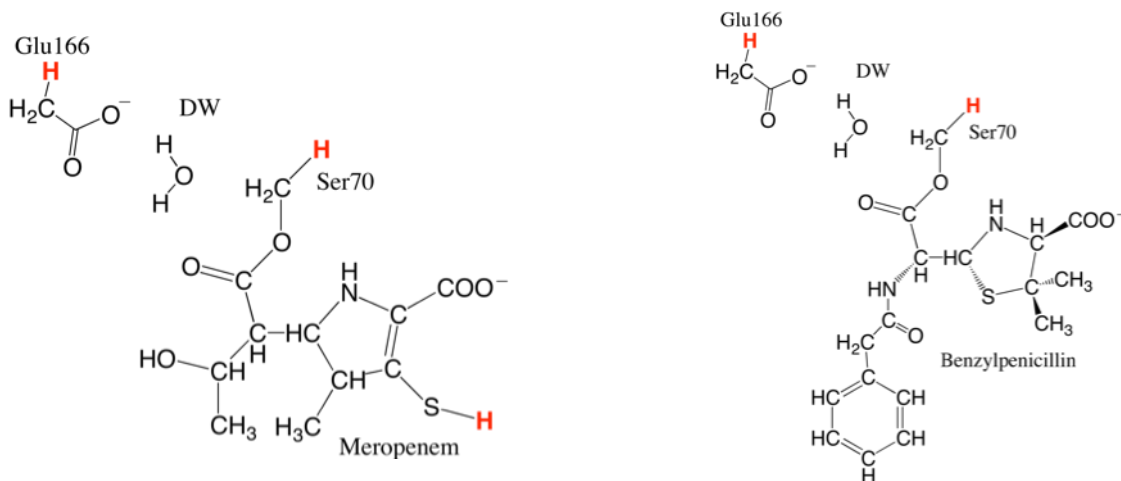


Figure S1. QM region used for QMMM calculations performed with meropenem (left) and benzylpenicillin (right).

A standard QM/MM equilibration protocol was used. This involved minimization, heating (in the NVT ensemble) and QM/MM MD in the NPT ensemble. First, unrestrained energy minimization was carried out for 1000 steps (100 steps Steepest Descent, 900 steps of Conjugate Gradient). This was followed by gradual heating from 50 K to 300 K in 50 ps (using Langevin dynamics for temperature control). Thereafter, an unrestrained 50 ps QM/MM MD equilibration at 300 K was performed in the NPT ensemble (1 ps pressure relaxation time). Thereafter, 300 ps unrestrained SCC-DFTB/ff12SB MD was carried out on the equilibrated acylenzyme complexes in the NPT ensemble, to study interactions in the acylenzyme and select suitable structures for umbrella sampling. All MD production runs were performed at 300 K and 1 atm with a 1 fs time-step; Langevin dynamics was used for temperature control (collision frequency 5 ps^{-1}) and pressure was controlled by coupling to an external bath (with a 5 ps pressure relaxation time). Throughout, SHAKE was applied to MM bonds involving hydrogen and a direct-space cut-off of 8 Å for non-bonded interactions with PME for long-range electrostatics was used.

Additional restraints were found to be required to keep simulations stable and avoid large conformational fluctuations. A restraint of $10 \text{ kcal}/(\text{mol } \text{Å}^2)$ force constant was applied when the distance between the amine hydrogen (of the five-membered ring) and the carbonyl oxygen exceeded 2.5 Å . Further, several distance restraints with a force constant of $50 \text{ kcal}/(\text{mol } \text{Å}^2)$ were applied when O-H or N-H distances of QM groups exceeded 1.2 Å , to avoid unwanted proton transfers (which were found to take place in initial test simulations).

QM/MM free energy profile calculations

The first step of deacylation was simulated as 2D free energy surface. The value of the reaction coordinate step was 0.1 Å , and 20 ps of MD was performed at each point. The calculated surfaces consisted of 204 and 374 points for the benzylpenicillin and meropenem simulations, and involved 4.08 ns and 7.48 ns of QM/MM MD, respectively.

The reaction coordinate approach was used to model the first step of the deacylation reaction. The proton transfer reaction coordinate was defined as: $r_x = d(\text{O}_{\text{Glu166}}-\text{H}_{2\text{DW}}) - d(\text{H}_{2\text{DW}}-\text{O}_{\text{DW}})$ (from 0.8 Å to -0.8 Å to facilitate the transfer of the proton from DW to Glu166). The DW nucleophilic attack on the β -lactam ring reaction coordinate was defined as: $r_y = d(\text{CC}_{\text{Mer/Benx}}-\text{O}_{\text{DW}})$, where CC represents the carbonyl carbon in meropenem or benzylpenicillin (from 3.5 Å to 1.4 Å for meropenem and from 2.5 Å to 1.4 Å for benzylpenicillin). Both reaction coordinates were incremented by 0.1 Å , and a restraint of $100 \text{ kcal mol}^{-1}\text{Å}^{-1}$ was used. 20ps of simulation was used for each umbrella sampling window. Once an initial scan along r_x was completed (with r_y fixed to the starting value), the structures produced at the end of these simulations were used as the starting point for a scan across r_y .

The simulations were performed under the same conditions as the QM/MM MD production simulations described above, and the reaction coordinate values were recorded every 1 fs. The harmonic distance restraints with a force constant of $100 \text{ kcal}/(\text{mol } \text{Å}^2)$ lead to well-overlapping umbrella sampling windows. With the recorded data, the

Weighted Histogram Analysis Method (WHAM)¹⁶ was used to calculate the potential of mean force, with 33 bins along r_x and 43 or 23 bins along r_y (for meropenem and benzylpenicillin, respectively) and a convergence tolerance of 5×10^{-7} kcal mol⁻¹.

Table S1. Crystal structures used for setup of QM/MM calculations with their PDB accession codes.

β -lactamase starting structure	PDB accession code
BlaC	3DWZ ⁸
CTX-M	1YLW ¹⁴
SHV-1	2ZD8 ⁹
TEM-1	1BT5 ¹⁰
KPC-2	2OV5 ¹¹
NMC-A	1BUE ¹²
SFC-1 Glu166Ala	4EV4 ⁷
SME-1	1DY6 ¹³
TEM-1/benzylpenicillin	1RQG ¹⁵

References

1. D.A. Case, T.A. Darden, T.E. Cheatham, III, C.L. Simmerling, J. Wang, R.E. Duke, R. Luo, R.C. Walker, W. Zhang, K.M. Merz, B. Roberts, S. Hayik, A. Roitberg, G. Seabra, J. Swails, A.W. Götz, I. Kolossváry, K.F. Wong, F. Paesani, J. Vanicek, R.M. Wolf, J. Liu, X. Wu, S.R. Brozell, T. Steinbrecher, H. Gohlke, Q. Cai, X. Ye, J. Wang, M.-J. Hsieh, G. Cui, D.R. Roe, D.H. Mathews, M.G. Seetin, R. Salomon-Ferrer, C. Sagui, V. Babin, T. Luchko, S. Gusarov, A. Kovalenko, and P.A. Kollman (2012), AMBER 12, University of California, San Francisco.
2. Wang, J.; Wolf, R.M.; Caldwell, J.W.; Kollman, P.A.; Case, D.A. Development and testing of a general Amber force field. *J. Comput. Chem.* 2004, 25, 1157–1174.
3. Gaussian 09, M. J. Frisch, G. W. Trucks, H. B. Schlegel, G. E. Scuseria, M. A. Robb, J. R. Cheeseman, G. Scalmani, V. Barone, B. Mennucci, G. A. Petersson, H. Nakatsuji, M. Caricato, X. Li, H. P. Hratchian, A. F. Izmaylov, J. Bloino, G. Zheng, J. L. Sonnenberg, M. Hada, M. Ehara, K. Toyota, R. Fukuda, J. Hasegawa, M. Ishida, T. Nakajima, Y. Honda, O. Kitao, H. Nakai, T. Vreven, J. A. Montgomery, Jr., J. E. Peralta, F. Ogliaro, M. Bearpark, J. J. Heyd, E. Brothers, K. N. Kudin, V. N. Staroverov, R. Kobayashi, J. Normand, K. Raghavachari, A. Rendell, J. C. Burant, S. S. Iyengar, J. Tomasi, M. Cossi, N. Rega, J. M. Millam, M. Klene, J. E. Knox, J. B. Cross, V. Bakken, C. Adamo, J. Jaramillo, R. Gomperts, R. E. Stratmann, O. Yazyev, A. J. Austin, R. Cammi, C. Pomelli, J. W. Ochterski, R. L. Martin, K. Morokuma, V. G. Zakrzewski, G. A. Voth, P. Salvador, J. J. Dannenberg, S. Dapprich, A. D. Daniels, Ö. Farkas, J. B. Foresman, J. V. Ortiz, J. Cioslowski, and D. J. Fox, Gaussian, Inc., Wallingford CT, 2009.
4. Vanquelef, E.; Simon, S.; Marquant, G.; Garcia, E.; Klimerak, G.; Delepine, J. C.; Cieplak, P.; Dupradeau, F.-Y. *Nucl. Acids Res.* 2011, 39, 511–517.
5. Søndergaard, C. R.; Olsson, M. H. M.; Rostkowski, M.; Jensen, J. H. *J. Chem. TheoryComput.* 2011, 7, 2284–2295.
6. W. L. Jorgensen, J. Chandrasekhar, J. D. Madura, R. W. Impey, and M. L. Klein. *J. Chem. Phys.* 1983, 79, 926.
7. F. Fonseca, E. I. Chudyk, M. W. van der Kamp, A. Correia, A. J. Mulholland, and J. Spencer. The Basis for Carbapenem Hydrolysis by Class A β -Lactamases: A Combined Investigation using Crystallography and Simulations. *J. Am. Chem. Soc.* 2012, 134, 18275–18285.
8. J.-E. Hugonnet, L. W. Tremblay, H. I. Boshoff, r. Barry, Clifton E, and J. S. Blanchard. Meropenem-clavulanate is effective against extensively drug-resistant Mycobacterium tuberculosis. *Science* 2009, 323, 1215–1218.
9. M. Nukaga, C. R. Bethel, J. M. Thomson, A. M. Hujer, A. Distler, V. E. Anderson, J. R. Knox, and R. A. Bonomo. Inhibition of Class A β -Lactamases by Carbapenems: Crystallographic Observation of Two Conformations of Meropenem in SHV-1. *J. Am. Chem. Soc.* 2008, 130, 12656–12662.
10. L. Maveyraud, L. Mourey, L. P. Kotra, J.-D. Pedelacq, V. Guillet, S. Mobashery, and J.-P. Samama. Structural Basis for Clinical Longevity of Carbapenem Antibiotics in the Face of Challenge by the Common Class A β -Lactamases from the Antibiotic-Resistant Bacteria. *J. Am. Chem. Soc.* 1998, 120, 9748–9752.
11. W. Ke, C. R. Bethel, J. M. Thomson, R. A. Bonomo, and F. van den Akker. Crystal Structure of KPC-2: Insights into Carbapenemase Activity in Class A β -Lactamases. *Biochem.* 2007, 46, 5732–5740.

12. P. Swaren, L. Maveyraud, X. Raquet, S. Cabantous, C. Duez, J.-D. Pedelacq, S. Mariotte-Boyer, L. Mourey, R. Labia, M.-H. Nicolas-Chanoine, P. Nordmann, J.-M. Frere, and J.-P. Samama. X-ray Analysis of the NMC-A β -Lactamase at 1.64-Å Resolution, a Class A Carbapenemase with Broad Substrate Specificity. *J. Biol. Chem.* 1998, 273, 26714–26721.
13. W. Sougakoff, G. L'Hermite, L. Pernot, T. Naas, V. Guillet, P. Nordmann, V. Jarlier, and J. Delettre. Structure of the imipenem-hydrolyzing class A β -lactamase SME-1 from *Serratia marcescens*. *Acta Crystallogr. D Biol. Crystallogr.* 2002, 58, 267–274.
- 14 Y. Chen, J. Delmas, J. Sirot, B. Shoichet, and R. Bonnet. Atomic Resolution Structures of CTX-M β -Lactamases: Extended Spectrum Activities from Increased Mobility and Decreased Stability. *J. Mol. Biol.* 2005, 348, 349–362.
- 15 N.C. Strynadka., H. Adachi, S.E Jensen, K. Johns, A. Sielecki, C. Betzel, K. Sutoh, M.N. James, Molecular Structure of acyl-enzyme intermediate in beta-lactam hydrolysis at 1.7 Å resolution, *Nature* 1992, 359, 700-705.
16. S. Kumar, J. M. Rosenberg, D. Bouzida, R. H. Swendsen, and P. A. Kollman. The weighted histogram analysis method for free-energy calculations on biomolecules. I. The method. *J. Comput. Chem.* 1992, 13, 1011–1021.

Free Energy Surfaces for carbapenem-inhibited β -lactamases with meropenem

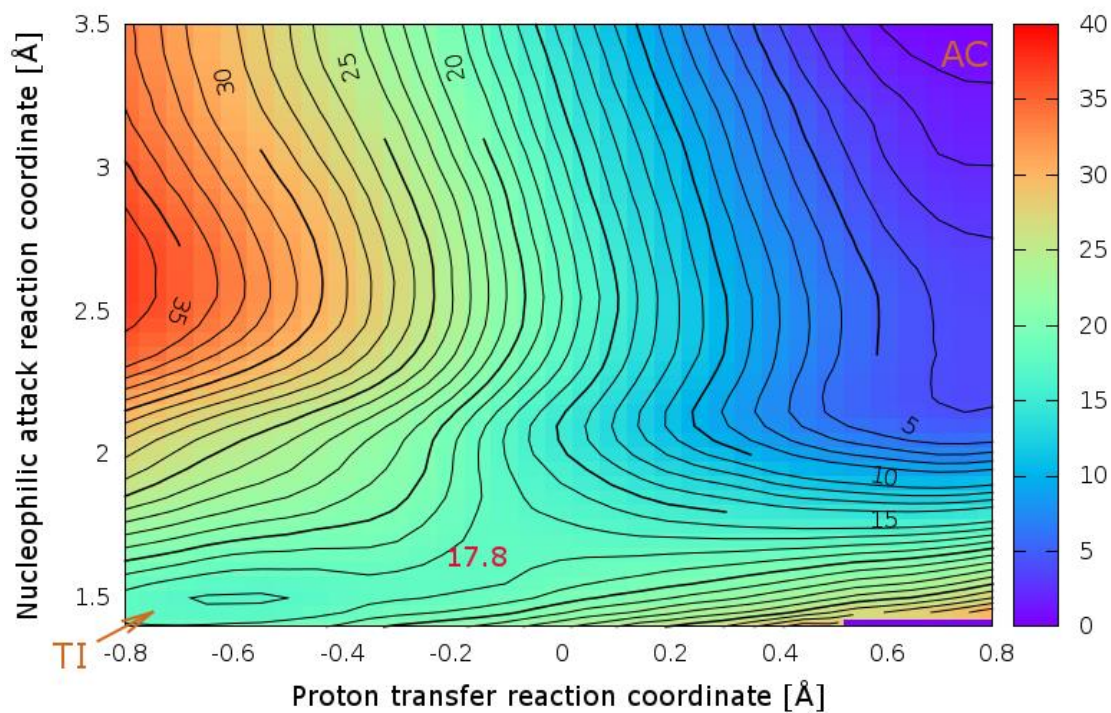


Figure S2. SCC-DFTB/ff12SB Free Energy Surface obtained by the Weighted-Histogram Analysis Method from umbrella sampling QM/MM MD simulations for BlaC with meropenem.

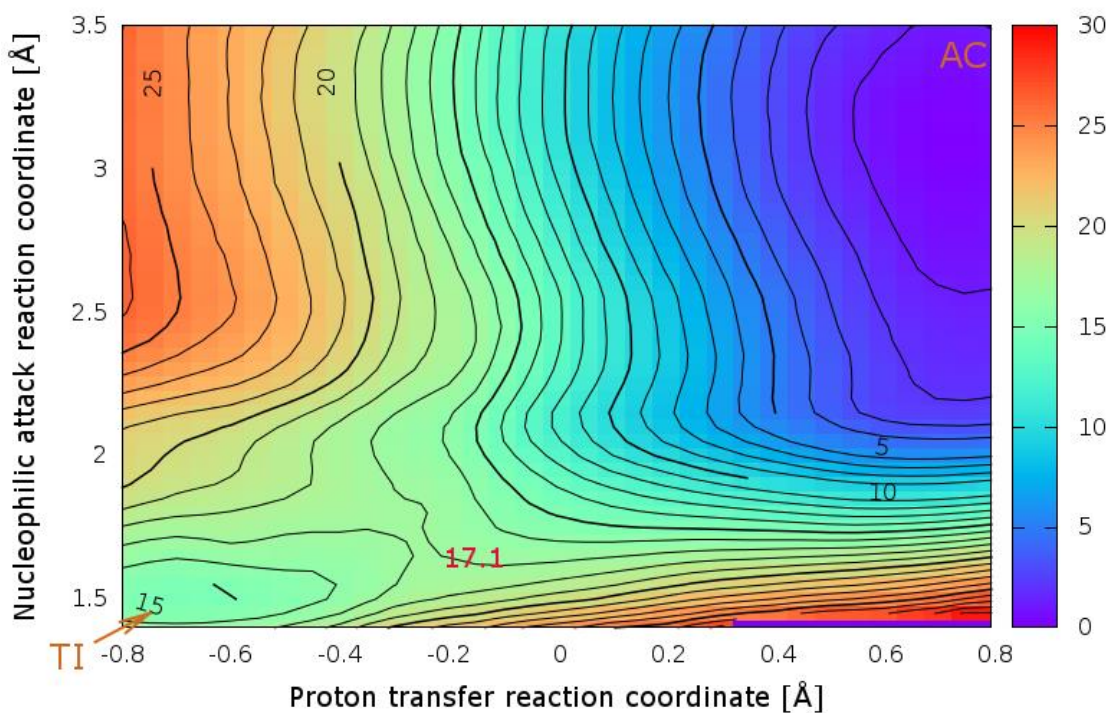


Figure S3. SCC-DFTB/ff12SB Free Energy Surface obtained by the Weighted-Histogram Analysis Method from umbrella sampling QM/MM MD simulations for SHV-1 with meropenem.

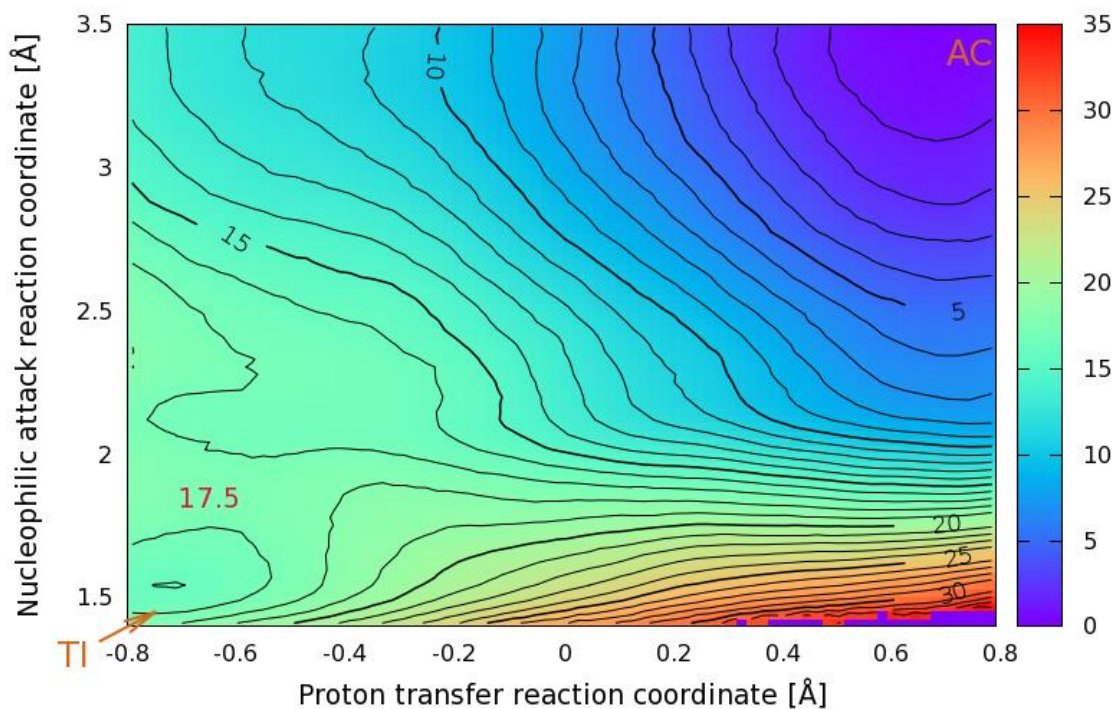


Figure S4. SCC-DFTB/ff12SB Free Energy Surface obtained by the Weighted-Histogram Analysis Method from umbrella sampling QM/MM MD simulations for TEM-1 with meropenem.

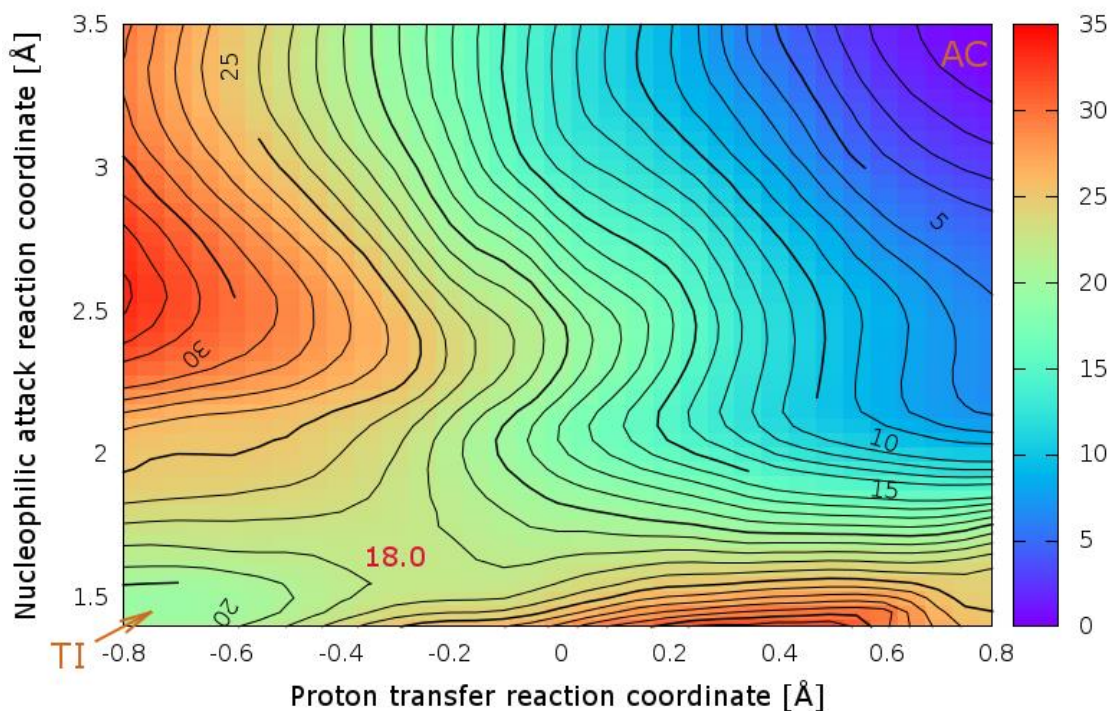


Figure S5. SCC-DFTB/ff12SB Free Energy Surface obtained by the Weighted-Histogram Analysis Method from umbrella sampling QM/MM MD simulations for CTX-M with meropenem.

Free Energy Surfaces for carbapenemases with meropenem

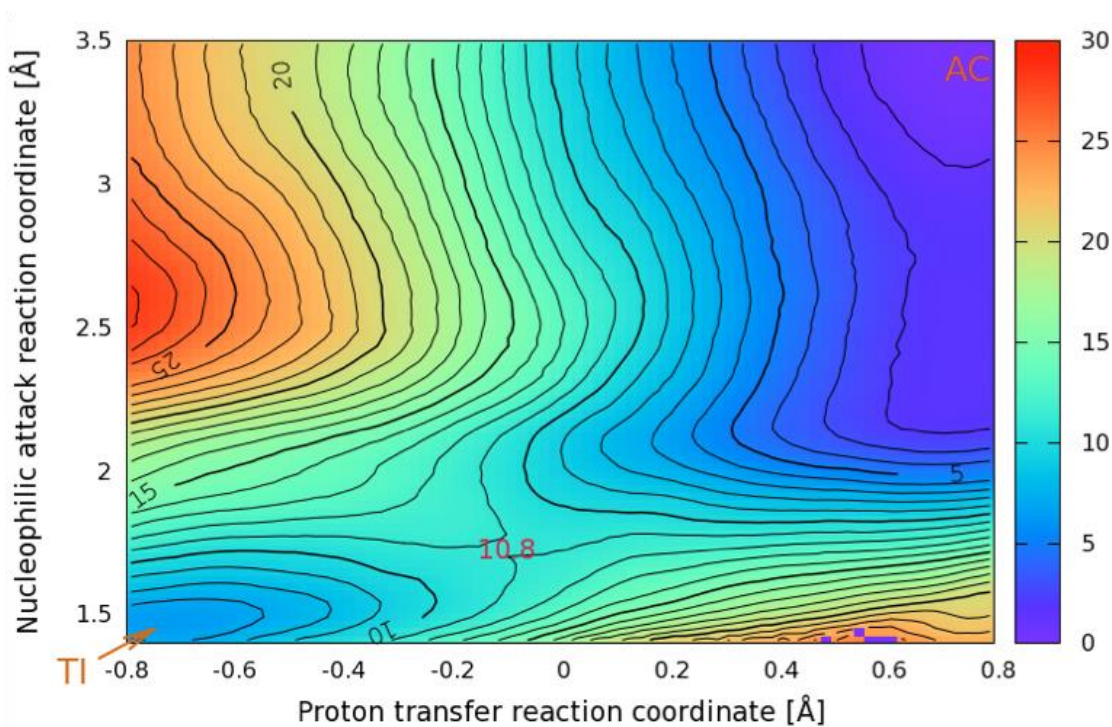


Figure S6. SCC-DFTB/ff12SB Free Energy Surface obtained by the Weighted-Histogram Analysis Method from umbrella sampling QM/MM MD simulations for KPC-2 with meropenem.

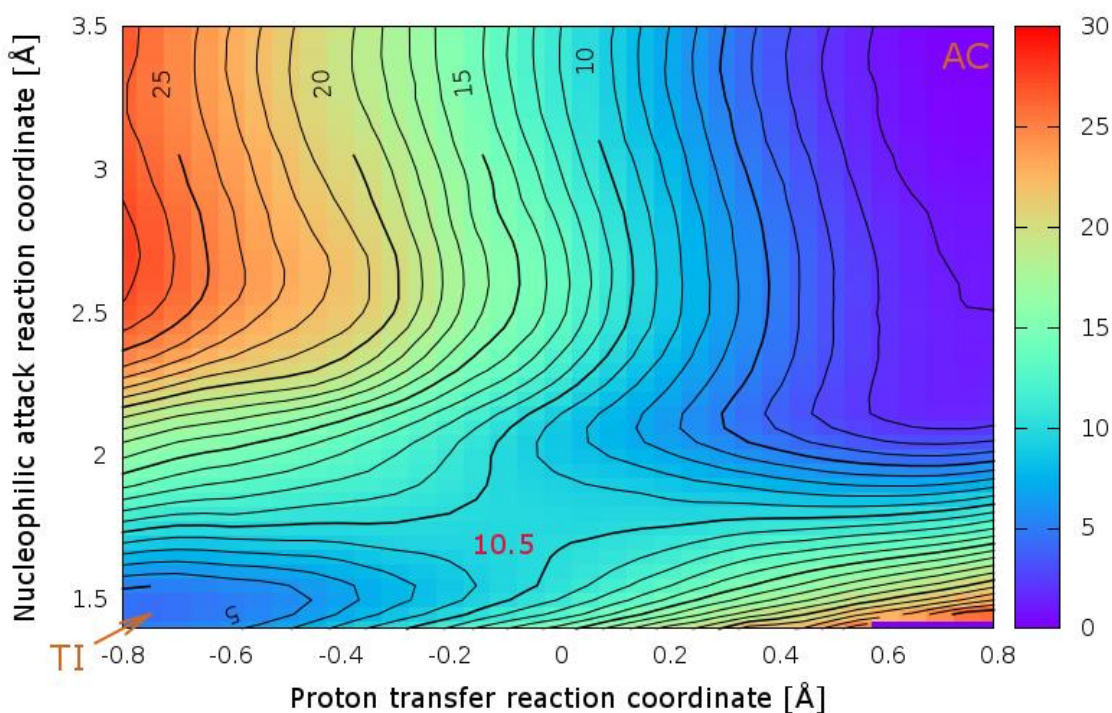


Figure S7. SCC-DFTB/ff12SB Free Energy Surface obtained by the Weighted-Histogram Analysis Method from umbrella sampling QM/MM MD simulations for SFC-1 with meropenem.

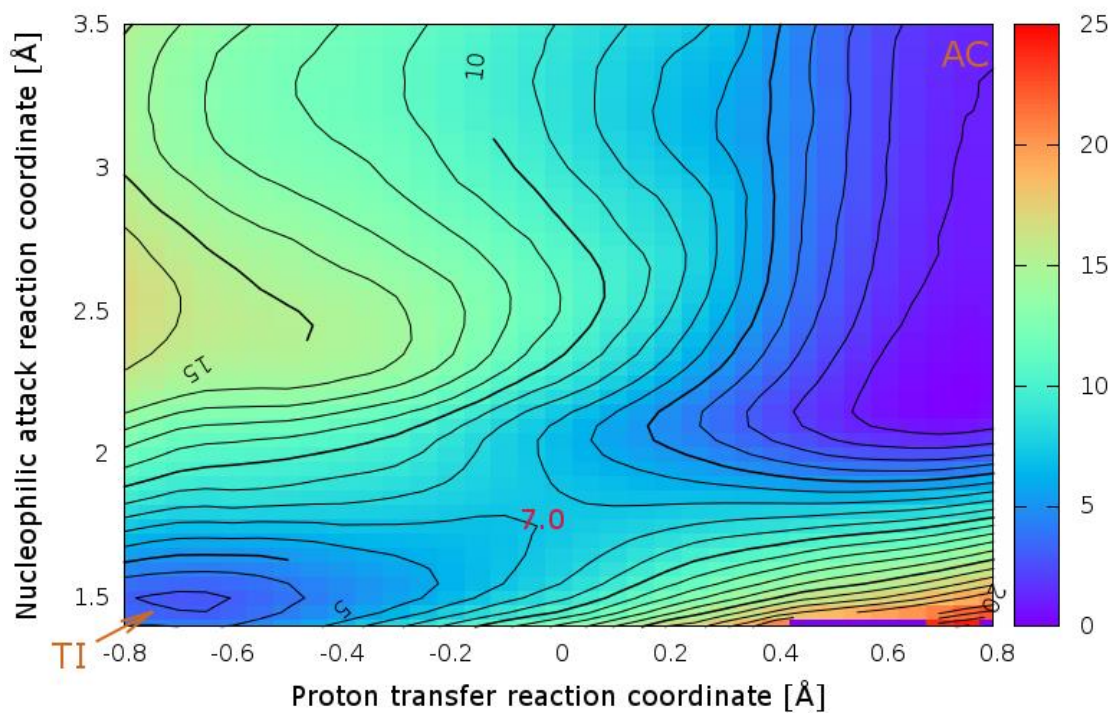


Figure S8. SCC-DFTB/ff12SB Free Energy Surface obtained by the Weighted-Histogram Analysis Method from umbrella sampling QM/MM MD simulations for NMC-A with meropenem.

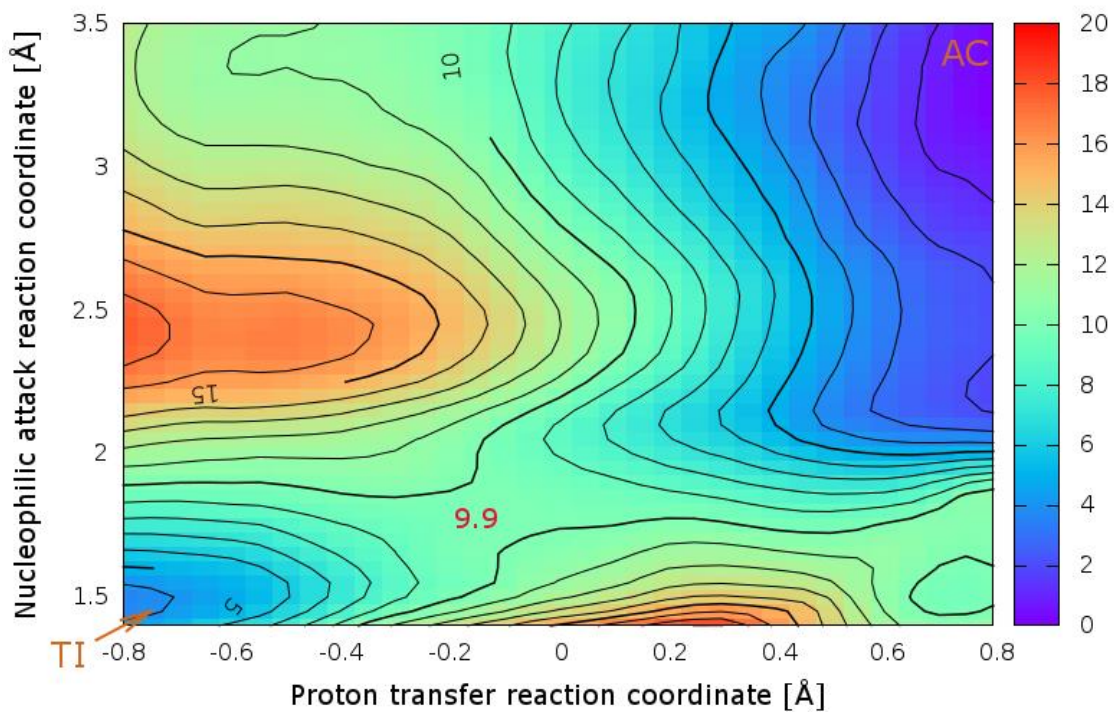


Figure S9. SCC-DFTB/ff12SB Free Energy Surface obtained by the Weighted-Histogram Analysis Method from umbrella sampling QM/MM MD simulations for SME-1 with meropenem.

Free Energy Surface for TEM-1 with benzylpenicillin

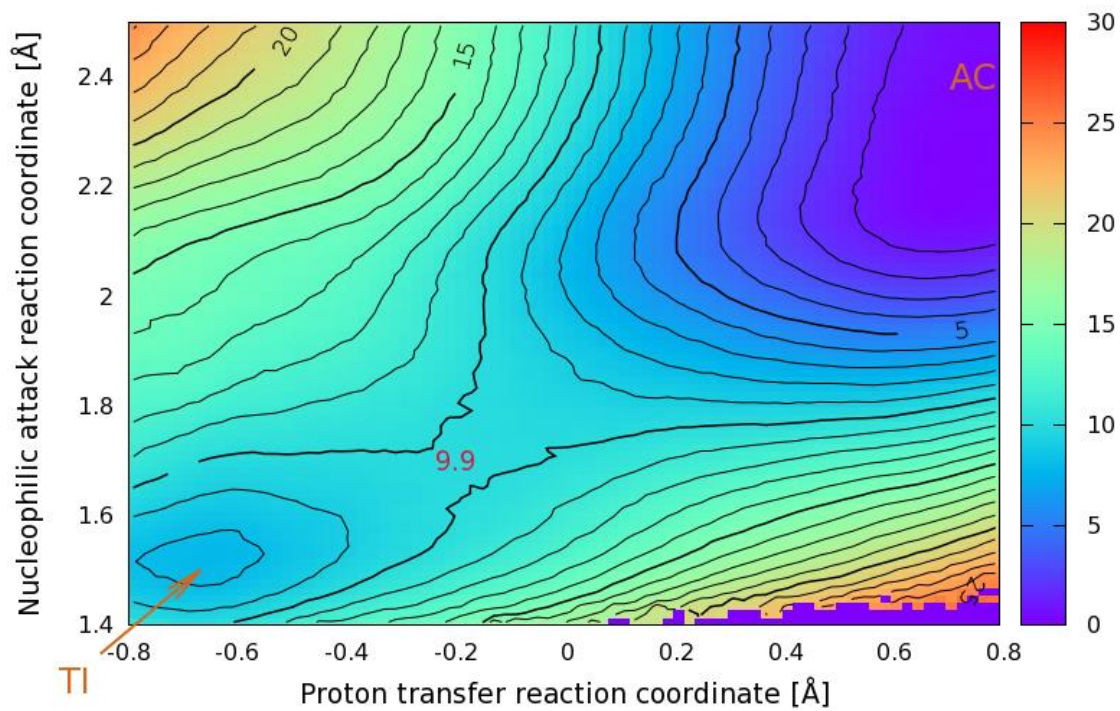


Figure S10. SCC-DFTB/ff12SB Free Energy Surface obtained by the Weighted-Histogram Analysis Method from umbrella sampling QM/MM MD simulations for TEM-1 with benzylpenicillin.